Brazilian Journal
of Chemical
Engineering

ISSN 0104-6632
Printed in Brazil
www.abeq.org.br/bjche

Vol. 34, No. 01, pp. 183 - 191, January - March, 2017
dx.doi.org/10.1590/0104-6632.20170341s20150681

THE FORMATION BEHAVIOR OF A SINGLE BUBBLE IN POWER-LAW FLUIDS

Shaobai Li, Shuang Xu, Zheng Yan, Rundong Li* and Tianhua Yang

Liaoning Key Laboratory of Clean Energy and School of Energy and Environment,
Shenyang Aerospace University, Shenyang, 110136, China.
E-mail: rdlee@163.com

(Submitted: October 26, 2015 ; Revised: December 24, 2015 ; Accepted: January 4, 2016)

Abstract - The formation behavior of a single bubble in power-law fluids (carboxymethyl cellulose solution, CMC) and Newtonian fluids (glycerol solution) was experimentally investigated via a high-speed camera. The effects of liquid property, orifice diameter and gas flow rate on bubble volume and aspect ratio were observed. It was found that the formation time and detaching volume increased with the increase of fluid viscosity. The increase of bubble aspect ratio during the bubble formation process was complex, with main emphasis on the decrease in the initial stage and an increase in the final stage along with the shear thinning property variation. Nevertheless, the bubble detaching volume, instantaneous volume and formation time increased following the increase of orifice diameter and gas flow rate. On the contrary, the bubble aspect ratio decreased with the orifice diameter increase but increased with a higher gas flow rate.
Keywords: Bubble formation; Power-law fluids; Rheological property; Bubble volume; Aspect ratio.

INTRODUCTION

The bubble motion in liquid phases is broadly encountered in many industrial processes, such as chemical, biochemical, mineral and environmental processes (Chhabra, 2006; Li *et al*., 2012). In these processes, the formation behavior of bubbles has aroused wide concern due to its influence on bubble volume, velocity, gas holdup and residence time, which can further affect the mass transfer, heat transfer and chemical reactions between gas-liquid phases (Plesset *et al*., 2003). Thus, a profound understanding of the bubble formation process in liquid phases is essential for optimizing the design of gas-liquid equipment, and significant efforts have been devoted in the last few decades. The earliest studies on the formation of a single bubble can be found in the work of Bashforth *et al*. (1883). Afterwards, numerous experimental and numerical simulation studies on bubble formation have been undertaken. In the 1970s, Kumar *et al*. (1970) studied the mechanism of bubble formation under different operational conditions. Tsuge *et al*. (1986) conducted the hydrodynamics of bubble formation from single orifices and discussed various proposed models for the process of bubble formation. Zhang *et al*. (2001) explored bubble formation and interaction on a plate orifice, and Gnyloskurenko *et al*. (2003) investigated the effect of wettability of the orifice on bubble formation. In the study of Pamperin *et al*. (1995), it is reported that the bubble departure diameter was proportional to the capillary diameter under micro-gravity circumstances. Kulkarni *et al*. (2005) reviewed the progresses and advancements on the research of bubble formation up to 2005, in which most of the proposed models for bubble formation are included and the effect of various system properties on various growth phases in the process are keenly discussed. More recently, Vakhshouri *et al*. (2009) examined the effects of the plenum chamber volume on bubble formation frequency, initial bubble size, and orifice velocity fluctuations, and hence developed a two-stage mechanistic model for bubble formation

*To whom correspondence should be addressed

at a single orifice submerged in a gas–solid fluidized bed. Xie *et al*. (2012) experimentally investigated the formation and detachment of the bubbles generated from an immersed micro-orifice on a plate in a stagnant and isothermal liquid. In addition to the experimental investigation, many researchers are dedicated to simulating the process of bubble formation by the direct numerical simulation (DNS) technique with prosperous computational methodology (Gerlach *et al*., 2007; Ma *et al*., 2012; Albdawi *et al* 2003; Wielhorski *et al*., 2014; Zahedi *et al*., 2014; Islam *et al*., 2015; Chakraborty *et al*. 2015).

These prior studies generally focused on Newtonian fluids, whereas it should be recognized that most fluids encountered in many industrially important applications (such as polymer, food, sewage sludge, slurries, and fermentation) display various non-Newtonian characteristics, including shear-thinning, shear-thickening, yield stress and viscoelastic characteristics (Chhabra *et al*., 2006). Despite their wide occurrence in diverse industrial applications, much less is known for bubble formation in non-Newtonian fluids due to their complicated rheological properties. Nevertheless, few studies have reported on the formation mechanism of bubbles in non-Newtonian fluids in spite of these inherent difficulties. The evolution of single bubble detaching volume under various operating conditions has been observed in early studies, with some simplified models for the bubble detaching volume established (Acharya *et al*., 1978; Teraska *et al*., 1991; Miyahara *et al*., 1988). On the basis of a force balance analysis, Li *et al*. (2002) developed a novel theoretical model for the non-spherical bubble formation at an orifice submerged in a non-Newtonian fluid by introducing the effects of inline interactions between two consecutive bubbles. Fan *et al*. (2014) numerically investigated the bubble generation in non-Newtonian fluids using the CLSVOF method and evaluated the variation of bubble volume and aspect ratio.

The power-law fluid is a typical type of non-Newtonian fluid, the apparent viscosity variation of which could be described by a power-law model. Moreover, this non-Newtonian fluid has multiple applications. For example, it can play the role of thickener in the food industry, or be employed as polymer-flooding agent in order to enhance oil recovery. This study was undertaken to determine the influence of several noteworthy variables, including fluid rheological properties, gas flow rate and orifice diameter, on the bubble formation in Newtonian and power-law fluids. By means of a high-speed digital camera, the instantaneous volume, detaching volume and shape of the bubble were recorded along with the bubble formation process in a single orifice. The results of this study are expected to extend the understanding of the factors affecting bubble formation and to be conducive to offering some insight into optimization of related process.

EXPERIMENTAL

Apparatus

The studies of bubble formation in power-law fluids were carried out using the experimental set-up shown in Figure 1. The principal part of the bubble formation system was a rectangular bubble column with a size of 0.15 m×0.15 m×50 m. On this scale, the wall effect on bubble formation can be neglected according to our previous research (Li *et al*., 2012). Nitrogen was injected via an orifice at the bottom of the bubble column from a gas cylinder by valve and rotameter (within ±0.01 cm^3/s). The orifices were made of 1 mm thick stainless steel. The inner diameters of the orifices used in the experiments were 1.0 mm, 1.6 mm and 2.4 mm, respectively. Three different gas-flow rates, 0.2 ml/s, 0.6 ml/s and 1.0 ml/s, were investigated. The bubble formation process was determined using a high-speed camera (Motion Pro Y5, REDLAKE Global USA) with a lens (Nikon, 24-85 mm/f2.8-4). In this work, the process of bubble formation was captured at a rate of 100 frames/s with the resolution of 500×1728 pixels. The selected sequence of frames was analyzed using Matlab 6.0 with a self-written code. All experiments were carried out at room temperature under constant pressure.

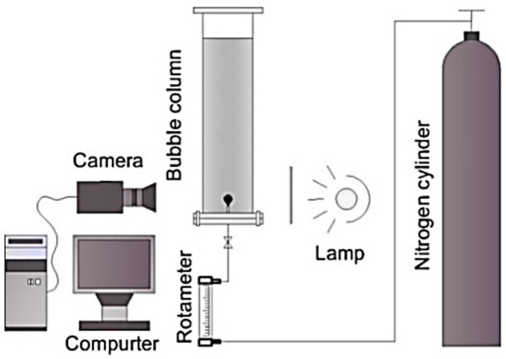

Figure 1: The experimental apparatus for bubble formation.

Materials

In this paper, nitrogen with purity of 99.9 vol. % was used as the gas phase. Glycerin aqueous solution

(50 wt %) was used as the referenced Newtonian fluid. CMC aqueous solutions with different concentration (0.35 wt %, 0.5 wt % and 0.7 wt %) were used as the referenced power-law fluids. Densities of the liquids were measured using a density meter (AntonPaar, DMA5000, Austria) with an accuracy of ±1.0%. The rheological properties were determined using a programmatic rheometer (Brookfield, DV-III, USA) with shear rate ranging from 0.1 to 1000 s^{-1}. The results are shown in Figure 2. From Figure 2, it can be observed that CMC solutions show shear thinning behavior. The variation of the apparent viscosity with shear rate could be described by the power-law model (Carreau *et al*., 1972):

$$\mu = K\dot{\gamma}^{n-1} \tag{1}$$

where K is the consistency index and n presents the flow index.

The physical properties of the experimental fluids are listed in Table 1.

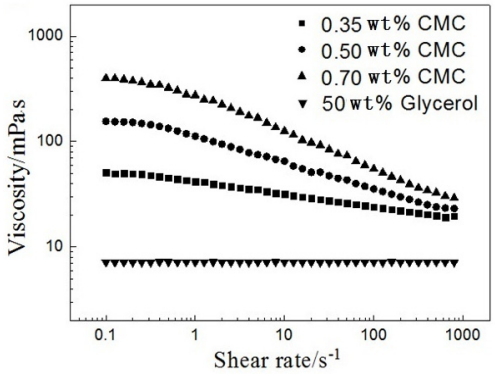

Figure 2: Rheological characteristics of the liquids used.

Table 1: Rheological and physical properties of the experimental fluids.

Concentration (wt %)	K ($mPa \cdot s^n$)	n	σ ($mN \cdot m^{-1}$)	ρ ($kg \cdot m^{-3}$)
0.35 **wt %** CMC	41.72	0.88	56.32	1002.63
0.50 **wt %** CMC	112.37	0.75	58.68	1004.82
0.70 **wt %** CMC	288.53	0.64	63.46	1009.31
50 **wt %** Glycerol	7.14	1	55.81	1131.24

THE FORCES ACTING ON A BUBBLE IN THE FORMATION PROCESS

The motion behavior of bubbles in the liquid phase is the result of the combination of diverse forces acting on the bubble, such as buoyancy, inertia force, surface tension, gravity force, the force from other bubbles, the forces from the liquid phase and forces from solid interfaces. However, the influence of forces on the bubble volume, formation time and bubble shape are different. The theoretical description of those forces is stated as follows:

Buoyancy:

$$F_B = V\left(\rho_l - \rho_g\right)g = V\rho_l g \tag{2}$$

where, V is the volume of the bubble, ρ_l and ρ_g are the density of the liquid phase and gas phase, respectively, and g is the gravitational acceleration.

Adhesive force of the orifice:

$$F_o = \pi D_o \sigma \tag{3}$$

where, D_o is the diameter of the bubble, and σ is the surface tension of the liquids.

The force of gas flow momentum:

$$F_M = \rho_g \frac{Q^2}{(\pi/4)D_O^2} \tag{4}$$

where, Q is the gas flow rate.

Bubble gravity:

$$F_G = m_b g = (11/96)\rho_l g \pi d^3 \tag{5}$$

where, d is the diameter of the bubble.

Drag force:

$$F_D = C_D \frac{\pi}{8}\rho d^2 U_b^2 \tag{6}$$

where U_b is the velocity of the bubble centre, and C_D is the drag coefficient of the bubble.

In low Reynolds number, the bubble drag coefficient could be expressed as $C_D = 16/\mathrm{Re}$ according to Hadamard-Ribczynky (1962) theory. For power-law fluids, the Reynolds number of the bubble is defined as:

$$Re = \frac{\rho U_b^2}{K\left(\frac{U_b}{d}\right)^n} = \frac{\rho U_b^{2-n} d^n}{K} \tag{7}$$

The force due to the wake of the former bubble:

$$Fw = \frac{1}{2}\rho_l \frac{\pi}{4} d^2 C_D v_w^2 \tag{8}$$

where v_w is the wake velocity of the previous detached bubble.

In accordance with Schlichting's (1968) theory, the wake velocity profile of the leading bubble can be denoted as follows:

$$v_w = \frac{\pi C_{D1}}{2}\left(1 - \exp\frac{\rho U_{b1} d_2}{16\mu x}\right) \tag{9}$$

where U_{b1} is the velocity of the previous bubble, x is the distance from the base of the previous bubble. r is the radial distance from the centre of the leading bubble base. C_{D1} is the drag coefficient of the previous bubble. μ is the viscosity of the experimental fluids, which could be calculated by Eq. (1).

This bubble formation ends when the sum of detaching forces is larger than or equal to that of the attaching forces, which can be stated as:

$$F_B + F_M + F_W \geq F_G + F_D + F_O \tag{10}$$

The above listed forces mainly influence the bubble formation time, thus impacting the bubble volume. In the case of bubble shape, an extra surface tension should be included apart from the above-listed influencing forces. The surface tension of the bubble can be described as:

$$F_\sigma = 2\pi d\sigma \tag{11}$$

RESULTS AND DISCUSSION

The Bubble Formation Process

Figure 3 shows the sequence of bubble formation in the Newtonian fluid (Figure 3a) and shear-thinning fluids (Figure 3b) with the conditions of Q=0.6 ml/s and D_o=2.0 mm. The evolution is recorded at the moment when the gas–liquid interface just stands out on the orifice, and this is defined as the initial bubble growth point. It can be seen from Figure 3 that the main period of bubble formation could be divided into three remarkable stages: bubble nucleation, bubble growth and necking. Although the mechanisms of bubble evolution are similar regardless of Newtonian fluid or shear-thinning fluids, differences in bubble shape and volume during the stages are revealed. During the nucleation stage, the bubble emerges from the orifice in the form of a spherical segment, which transforms into part of a sphere while its periphery remains constant. As to the bubble growth stage, the bubble then expands greatly in length and radial direction, and the shape varies in different fluids. In the case of 50 wt% glycerol solution, bubble configuration remains part of a sphere-like shape while its base attaches to the orifice. However, the bubble becomes elongated in the 0.5 wt% CMC solution, and then expands while moving upwards, followed by substantial

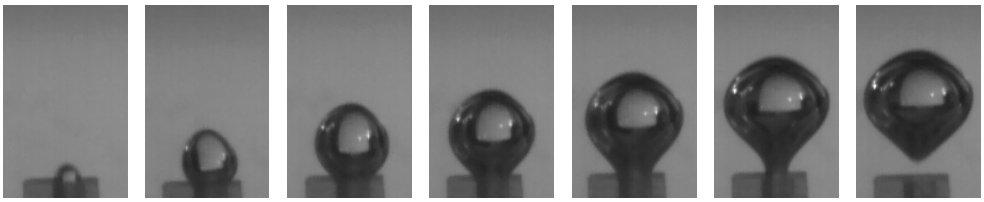

T=0 s *T* =0.05 s *T* =0.1s *T* =0.15 s *T* =0.21 s *T* =0.26 s *T* =0.32 s

(a: 50 wt% Glycerol)

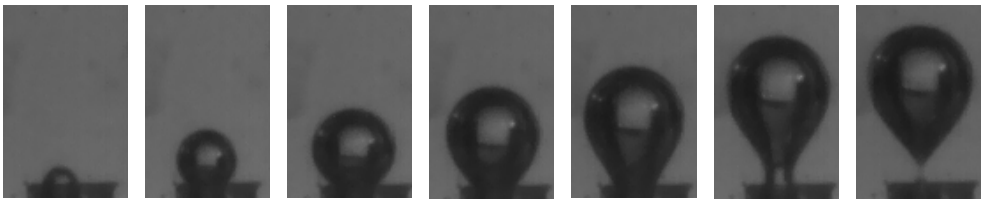

T =0 s *T* =0.07 s *T* =0.14 s *T* =0.21 s *T* =0.28 s *T* =0.34 s *T* =0.41 s

(b: 0.5 wt% CMC)

Figure 3: Series of instantaneous states of bubble formation in the experimental liquids.

distortion of the bubble configuration in comparison with a spherical shape. In the final necking stage, additional gas is fed into the bubble, leading to the continuous growth in bubble size. The bubble lifts away from the orifice, but is still attached to it through a neck, which also grows with time. When the sum of detaching forces is larger than or equal to that of the attaching forces, the neck is cut off and the bubble detaches.

The differences in bubble shape evolution can be attributed to the different rheological properties of glycerol solution and CMC solutions. It can be observed from Figure 2 that CMC solutions show noticeable shear thinning behavior. Li *et al*. (1997) simulated the passage of bubbles by exerting consecutive shear rates of glycerol solutions and CMC solutions in a rheometer. They found that, after the passage of a leading bubble, the memory effect of CMC solutions held the shear-thinning process for a certain period, which results in the decrease in local viscosity of the previous bubble wake. Nevertheless, this effect is not expected to occur in a Newtonian fluid. Therefore, the decrease in the viscosity of the previous bubble wake can influence the formation of following bubbles by two aspects. On the one hand, it increases the force due to the wake of the previous bubble (i.e., $F_w = \frac{1}{2}\rho_1 \frac{\pi}{4} d^2 C_D v_w^2$). Besides, it decreases the viscous resistance right above the bubble. Accordingly, the bubble shape formed in CMC solutions is more elongated than that in Newtonian fluids.

The Influence of Liquid Rheological Properties

The bubble formation process in different fluids with Q=0.6 ml/s and D_O=2.0 mm were conducted as shown in Figure 4. It can be seen that, except for the formation time and detaching volume, the variation of bubble instantaneous volume displays a less pronounced change for different fluids during the formation process, although the variation curves of bubble volume with time slightly intersect. This trend is consistent with the report of Acharya *et al* (1978). The slight intersecting of variation curves could be explained by the difference in surface tension of the tested fluids. As the bubble starts to generate, the gas flow must be against the liquid film of the orifice, the strength of which depends on the surface tension of the fluids. It can be found from Table 1 that the surface tension of 50 wt% glycerol is the lowest of the tested fluids, and the surface tension of CMC solutions increases with increasing CMC concentration, but the difference is quite slight due to the small surface tension margin of the tested fluids. With the formation process approaching to the end, the bubble attaching to the orifice goes through a narrow neck, leading to a slower growth in bubble size. It can be seen from Figure 4 that the formation time of a bubble in 50 wt% glycerol is shorter than that in CMC solution, in which the formation time of the bubble increases with the increase of the solution concentration. Hence, the variation curves of bubble volume with time slightly intersect. Yet, it should also be noted that the distinctions in the bubble formation time and detaching volume in different fluids are apparent. For 50 wt% glycerol solution, the formation time is 0.32 s and the detaching volume is 135×10^{-9} m^3. As to 0.35 wt% CMC solution, the formation time and the detaching volume are 0.34 s and 155×10^{-9} m^3. When it comes to 0.50 wt% and 0.70 wt% CMC solution, the formation time and the detaching volume are 0.41 s and 183×10^{-9} m^3, 0.52 s and 230×10^{-9} m^3, separately. The bubble formation time and detaching volume are related to the viscosity of the solutions. As demonstrated in Figure 2, the viscosity of 50 wt% glycerol is lower than those of CMC solutions, and the viscosity of CMC solutions increases with increasing solution concentration in the shear rate ranging from 0.1 to 1000 s^{-1}. For a bubble rising in a liquid, the shear rate (ie U/d) is less than 100 s^{-1}(Li *et al*., 2012), thus for viscosity, 50 wt% glycerol＜0.35 wt% CMC＜0.50 wt% CMC＜0.70 wt% CMC. Martín *et al*. (2006) experimentally studied the influence of liquid viscosity on the bubble volume and formation time, and proposed that the velocity of the liquid layer of the gas-liquid interface must equal the velocity of the gas in its outer layer. As the viscosity increases, the velocity of the liquid layer is smaller, allowing the bubble to grow further until the bubble neck is cut. Additionally, an increase of the liquid viscosity is able to enhance the drag force (i.e. F_D) and reduce the force due to the wake of the former bubble (i.e., F_W). Hence, the bubble volume and formation time increase along with the elevation of liquid viscosity.

The sequence of instantaneous states of bubble formation in Figure 3 could only roughly describe the evolution of bubble shape. Therefore, the aspect ratio is introduced as follows in order to more precisely describe the bubble shape evolution in the formation process.

$$E = \frac{a}{b} \tag{12}$$

where b and a are the vertical diameter and horizontal diameter, respectively.

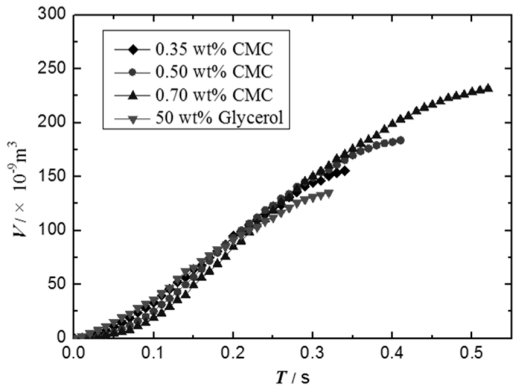

Figure 4: The variation of bubble volume with the liquid properties.

The influence of the liquid rheological properties on the variation of the bubble aspect ratio is presented in Figure 5. It is found that evolutions of the bubble shape in different liquids follow a similar tendency, by which the aspect ratios increase with prolonged time. For power-law fluids, the increase rate of the aspect ratio in the bubble nucleation stage declines as the concentration of the CMC solution increases, but shows an opposite trend along with the increase of the CMC solution concentration at the stage of bubble growth and necking. For 50 wt% glycerol solution, the aspect ratio initially increases rapidly with time, arriving at a maximum value (1.08) at 0.05 s. Afterwards, it falls to about 1.04 at 0.16 s, and then reaches about 1.1 at the detaching period. In the study of Xie *et al*. (2012), it was found that a time interval indeed exists between the former bubble departure and the following bubble formation. The gas phase space pressure gradually increases caused by the persistent gas supplement. Once the gas–liquid interface of the orifice is broken through and the gas is pushed up, a new bubble formation process will get started. The vertical velocity of gas is greater because of the inertia effect, and the vertical velocity of gas would gradually disappear due to the existence of the liquid viscosity. Therefore, in the bubble nucleation stage, the increase of the aspect ratio in 50 wt% glycerol solution is fastest owing to the lowest viscosity, and the rate decreases with the increase of CMC solution concentration. As the process goes forward, the vertical velocity of the gas vanishes, due to the viscosity force and a buffer of bubble intracavity, and the viscosity force and the surface tension gradually become dominating. With respect to 50 wt% glycerol solution, the viscosity and surface tension are constant in all directions. Hence, the increase of the aspect ratio is so slow that the bubble shape is nearly spherical in the bubble growth stage. On the contrary, the increase of aspect ratio of CMC solution exhibits a prompt trend with the concentration increasing at the stages of bubble growth. This distinction can be ascribed to the reduced viscosity of the liquid above the bubble, which is caused by the shear-thinning effect from the transformation of CMC concentration.

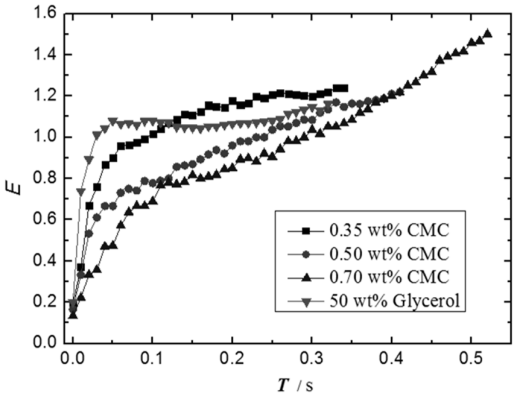

Figure 5: The variation of bubble aspect ratio with the fluid properties.

The Influence of Orifice Diameter

The comparison of bubble volume in 0.5 wt% CMC solution (Q=0.6 ml/s) with three different orifice diameters is shown in Figure 6. The orifice diameter shows a considerable effect on the bubble detaching volume and instantaneous volume. The bubble detaching volume, instantaneous volume and formation time increase with enlargement of the orifice diameter. As known from section 3.1, the force of gas flow and adhesive force of the orifice are closely associated with the orifice diameter. With increasing orifice diameter, the adhesive force of the orifice increases, whereas the detaching force of the gas flow decreases. Eventually, the change in the force status of the bubble during the formation process affects the bubble formation time. Meanwhile, the bubble detaching volume and instantaneous volume increase as well.

The influence of orifice diameter on bubble aspect ratio in 0.5 wt% CMC solution (Q=0.6 ml/s) is shown in Figure 7. It can be observed from Figure 7 that the bubble aspect ratio decreases with the increase of orifice diameter. On the basis of the conclusions drawn above, the smaller the orifice diameter, the shorter the bubble formation time, which means the frequency of the bubble generation escalates with smaller orifice diameter at the same gas flow rate. The bubble–bubble interactions are strengthened as well. In this case, the wake of the previous bubble has a greater influence on the generating bubble, by which F_w

increases. Meanwhile, the viscosity of the liquid on the top of the generated bubble is thinner than that of other area around the bubble. The result of the two impacts above gives rise to the bubble being more elongated with smaller orifice diameter.

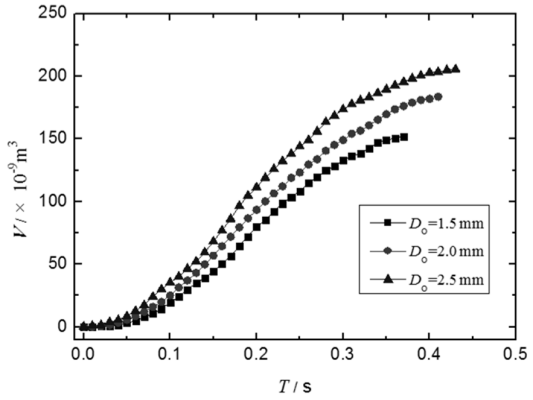

Figure 6: The variation of bubble volume with the orifice diameter.

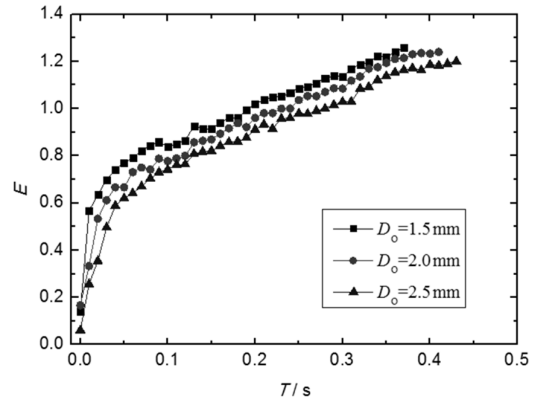

Figure 7: The variation of bubble aspect ratio with the orifice diameter.

The Influence of Gas Flow Rate

The bubble formation process for different gas flow rates with 0.5 wt% CMC solution and D_O=2.0 mm was performed as demonstrated in Figure 8. The bubble volume profile shows that, when the gas flow rate increases, the instantaneous and detachment volume of the bubble increase, but the bubble formation time significantly shortens. It should be noted that the density of gas phase can be considered to be constant in the process of bubble formation. Besides, the gas flow (F_M) and the force of the former bubble wake (F_W) increase with the rising gas flow, resulting in higher formation frequency and shorter formation time of the bubble. Nevertheless, both the instantaneous and detached volumes increase due to the high gas flow rate. The above results agree well with simulated results obtained by the VOF method (Fan *et al*., 2014).

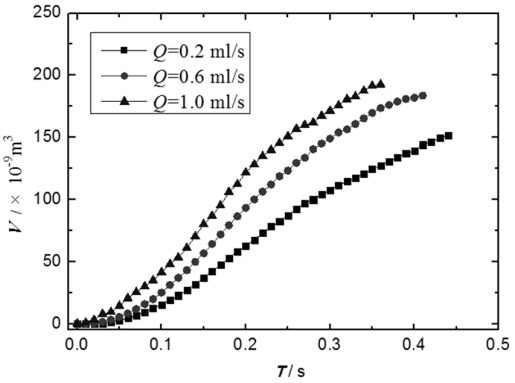

Figure 8: Influence of gas flow rate upon the bubble volume.

Figure 9 depicts the influence of gas flow rate upon the bubble aspect ratio. In Figure 9, it is observed that the bubble aspect ratio increases with increasing the gas flow rate. One of the crucial reasons is that the force of gas flow momentum (F_M in Eq. (4)) is strengthened along with the gas flow rate increase, which further promotes a bubble more stretched in the perpendicular direction. In addition, the former bubble wake (F_W) also increases owing to the increasing bubble generation frequency, which will result in the viscosity of the liquid above the forming bubble being thinner than that of other areas around the bubble.

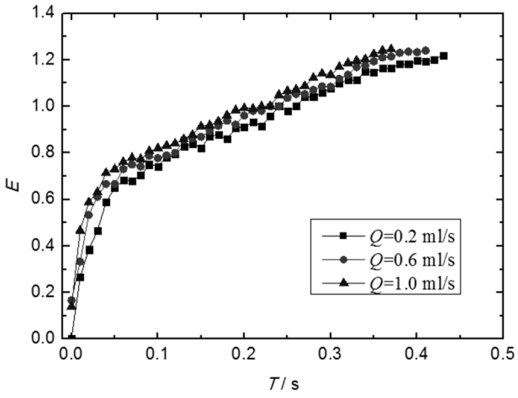

Figure 9: Influence of gas flow rate upon the bubble aspect ratio.

CONCLUSIONS

Bubble formation in shear-thinning fluids (CMC solutions of different concentration) and Newtonian fluids (50 wt% glycerol solution) at different orifice

diameters and gas flow rates were studied experimentally using a high-speed camera. The effects of the liquid property, gas flow rate and orifice diameter on volume variation and shape evolution were investigated respectively, from which the following conclusions were drawn.

(1) The bubble volume and formation time increase with the increase of fluid viscosity. The viscosity and rheological property play a notable role in bubble shape evolution. For 50 wt% glycerol solution, the increase of the aspect ratio is fastest owing to the low viscosity in the bubble nucleation stage, and then slowly declines, giving rise to the spherical bubble shape in the bubble growth stage. With regard to power-law fluids, the increase of the aspect ratio in the bubble nucleation stage decreases as the concentration of CMC solution increases at the bubble nucleation stage, and then presents an increase in the stages of bubble growth and necking due to the shear-thinning effect of CMC concentration.

(2) The orifice diameter greatly influences the bubble detaching volume and instantaneous volume. The bubble detaching volume, instantaneous volume and formation time increase significantly with enlargement of the orifice diameter. Besides, the bubble aspect ratio decreases as the orifice diameter increases.

(3) Both the instantaneous and detachment volume of the bubble increase when the gas flow rate rises, but the bubble formation time shortens obviously. The bubble aspect ratio shows an increasing tendency as well.

ACKNOWLEDGEMENTS

The project support by the National Natural Science Foundation of China (Grant No. 21406141), the Scientific Research Starting Foundation for Doctors of Liaoning Province, China (Grant No. 20141078) and the Research Foundation of Education Bureau of Liaoning Province, China (Grant No. L2014060) are gratefully acknowledged.

NOMENCLATURE

a	The horizontal diameter of bubble, (m)
b	the vertical diameter of bubble, (m)
C_D	drag coefficient, dimensionless
d	diameter of bubble, (m)
D_o	diameter of orifice, (m)
E	bubble aspect ratio
F_D	drag force, (N)
F_G	bubble gravity, (N)
F_M	the force of gas flow momentum, (N)
$F_\circ$	adhesive force of orifice, (N)
F_w	The force of the wake of the former bubble, (N)
g	gravity acceleration, ($m \cdot s^{-2}$)
K	consistency coefficient
m_b	bubble mass
n	flow index, (dimensionless)
Q	gas flow rate, ($m^3 \cdot s^{-1}$)
r	the radial distance from the center of the previous bubble base, (m)
Re	Reynolds number
T	Time, (s)
U_b	the velocity of the bubble center, ($m \cdot s^{-1}$)
U_{bl}	the velocity of the previous bubble, ($m \cdot s^{-1}$)
V	bubble volume, (m^3)
v_w	the wake velocity of the previous bubble, ($m \cdot s^{-1}$)
x	the distance from the base of the previous bubble, (m)

Greek Symbols

$\dot{\gamma}$	shear rate, (s^{-1})
μ	viscosity of liquid, (mPa·s)
ρ_g	gas density, ($kg \cdot m^{-3}$)
ρ_l	liquid density, ($kg \cdot m^{-3}$)
σ	surface tension, ($mN \cdot m^{-1}$)

REFERENCES

Acharya, A., Mashelkar, R. A., Ulbrecht, J. J., Bubble formation in non-Newtonian liquids. Industrial & Engineering Chemistry Fundamentals, 17, p. 230-232 (1978).

Albadawi, A., Donoghue, D. B., Robinson, A. J., Robinson, A. J., Murray, D. B., Delaure, Y. M. C., On the analysis of bubble growth and detachment at low capillary and bond numbers using volume of fluid and level set methods. Chemical Engineering Science, 90, p. 77-91 (2013).

Bashforth, F., Adams, J. C., An Attempt to Test the Theories of Capillary Action. Cambrige University Press, Cambridge (1883).

Carreau, Pierre, J., Rheological equations from molecular network theories. Journal of Rheology, 16, p. 99-127 (1972).

Chakraborty, I., Biswas, G., Polepalle, S., Ghoshdastidar, P. S., Bubble formation and dynamics in a

quiescent high-density liquid. AIChE Journal, 61(11), p. 3996-4012 (2015).

Chhabra, R. P., Bubbles, Drops, and Particles in Non-Newtonian Fluids. CRC Press (2006).

Davidson, J. F., Schuler, B. O. G., Bubble formation at an orifice in an inviscid liquid. Transactions of the Institution of Chemical Engineers, 38, p. 335-342 (1960).

Fan, W., Sun, Y., Chen, H., Bubble volume and aspect ratio generated in non-Newtonian fluids. Chemical Engineering & Technology, 37, p. 1566-1574 (2014).

Gerlach, D., Alleborn, N., Buwa, V., Durst, F., Numerical simulation of periodic bubble formation at a submerged orifice with constant gas flow rate. Chemical Engineering Science, 62, p. 2109-2125 (2007).

Gnyloskurenko, S. V., Byakova, A. V., Raychenko, O. I., Nakamura, T., Influence of wetting conditions on bubble formation at orifice in an inviscid liquid. Transformation of bubble shape and size. Colloids and Surfaces, A: Physicochemical and Engineering Aspects, 218, p. 73-87 (2003).

Islam, T., Ganesan, P., Sahu, J. N., Hamad, F. A., Numerical study to investigate the effect of inlet gas velocity and Reynolds number on bubble formation in a viscous liquid. Thermal Science, 19(6), p. 15-15 (2015).

Kulkarni, A. A., Joshi, J. B., Bubble formation and bubble rise velocity in gas-liquid systems: A review. Industrial & Engineering Chemistry Research, 44, p. 5873-5931(2005).

Kumar, R., Kuloor, N. R., The Formation of Bubbles and Drops. Adv. Chem. Eng., Academic Press, New York (1970).

Levich, V. G., Physicochemical Hydrodynamics. Prentice-Hall, Englewood Cliffs, NJ (1962).

Li, H. Z., Mouline, Y., Choplin, L., Funfschillinga, D., Marchala, P., Midouxa, N., Rheological simulation of in-line bubble interactions. AIChE Journal, 43, p. 265-267 (1997).

Li, H. Z., Mouline, Y., Midoux, N., Modelling the bubble formation dynamics in non-Newtonian fluids. Chemical Engineering Science, 57, p. 339-346 (2002).

Li, S., Ma, Y., Fu, T., Zhu, C., Li, H., The viscosity distribution around a rising bubble in shear-thinning non-Newtonian fluids. Brazilian Journal of Chemical Engineering, 29(2), p. 265-274 (2012).

Li, S., Ma, Y., Jiang, S., Fu, T., The drag coefficient and the shape for a single bubble rising in non-Newtonian fluids. Journal of Fluids Engineering, 134, p. 669-679 (2012).

Ma, D., Liu, M., Zu, Y., Tang, C., Two-dimensional volume of fluid simulation studies on single bubble formation and dynamics in bubble columns. Chemical Engineering Science, 72, p. 61-77 (2012).

Martin, M., Montes, F. J., Galan, M. A., On the influence of the liquid physical properties on bubble volumes and generation times. Chemical Engineering Science, 61, p. 5196-5203 (2006).

Miyahara, T., Wang, W. E. I. H., Takahashi, T., Bubble formation at a submerged orifice in non-Newtonian and highly viscous Newtonian liquids. Journal of Chemical Engineering of Japan, 21, p. 620-626 (1988).

Pamperin, O., Rath, H., Influence of buoyancy on bubble formation at submerged orifices. Chemical Engineering Science, 50, p. 3009-3024 (1995).

Plesset, M. S., Prosperetti, A., Bubble Dynamics and Cavitation. Annual Review of Fluid Mechanics, 9 p. 145-185 (2003).

Schlichting, H., Boundary Layer Theory. 6th Edn. McGraw-Hill, N.Y. (1968).

Terasaka, K., Tsuge, H., Bubble formation at a single orifice in non-Newtonian liquids. Chemical Engineering Science, 46, p. 85-93 (1991).

Tsuge, H., Hydrodynamics of Bubble Formation from Submerged Orifices. In: Encyclopaedia of Fluid Mechanics, Gulf Publishing Company: New York, Vol. 3, 191 (1986).

Vakhshouri, K., Grace, J. R., Modeling of bubble formation at a submerged orifice in a gas-fluidized bed. Chemical Engineering Research & Design, 87, p. 843-851 (2009).

Wielhorski, Y., Abdelwahed, A., Arquis, E., Numerical simulation of bubble formation and transport in cross-flowing streams. The Journal of Computational Multiphase Flows, 6, p. 299-312 (2014).

Xie, J., Zhu, X., Liao, Q., Wang, H., Ding, Y. D., Dynamics of bubble formation and detachment from an immersed micro-orifice on a plate. International Journal of Heat & Mass Transfer, 55, p. 3205-3213 (2012).

Zahedi, P., Saleh, R., Moreno-Atanasio, R., Yousefi, K., Influence of fluid properties on bubble formation, detachment, rising and collapse; Investigation using volume of fluid method. Korean Journal of Chemical Engineering, 31(8), p. 1349-1361 (2014).

Zhang, L., Shoji, M., Aperiodic bubble formation from a submerged orifice. Chemical Engineering Science, 56, p. 5371-5381 (2001).